0022-3565/97/2831-0293$03.00/0
THE JOURNAL OF PHARMACOLOGY AND EXPERIMENTAL THERAPEUTICS
Vol. 283, No. 1

Printed in U.S.A.
JPET 283:293–304, 1997

Kinetic Evidence for Active Efflux Transport across the Blood-Brain Barrier of Quinolone Antibiotics[1]

TSUYOSHI OOIE,[2] TETSUYA TERASAKI,[3] HIROSHI SUZUKI and YUICHI SUGIYAMA

Department of Pharmaceutics, Faculty of Pharmaceutical Sciences, The University of Tokyo, Bunkyo-ku, Tokyo 113, Japan

Accepted for publication June 10, 1997

ABSTRACT

A distributed model has been used to clarify the mechanism of the restricted and differential distribution of the quinolone antibiotics in the rat central nervous system (CNS). The symmetrical permeability clearances across the blood-brain barrier (BBB), PS_{BBB}, and across the blood-cerebrospinal fluid barrier (BCSFB), PS_{CSF}, and the active efflux clearances across the BBB, $PS_{BBB,eff}$, were obtained from a nonlinear least squares regression analysis combined with the fast inverse Laplace transforming program for *in vivo* data. The values of $PS_{BBB,eff}$ were 10- to 260-fold greater than those of PS_{BBB}, providing kinetic evidence to support the hypothesis that a significant efflux transport across the BBB is responsible for the limited distribution of quinolones in brain tissue. Moreover, by simulation studies, we could demonstrate the concentration profiles in the brain as a function of the distance from the ependymal surface. However, active efflux transport across the BCSFB has been suggested to have only a slight effect on the apparent elimination from the cerebrospinal fluid. Comparing the apparent brain tissue-to-unbound serum concentration ratio at steady state, it has been suggested that the net flux across the BBB, *i.e.*, the ratio of PS_{BBB} to the sum of PS_{BBB} and $PS_{BBB,eff}$, is a determinant for the differential distribution of these quinolones in brain tissue. Such a putative active efflux transport system would play a significant role in decreasing the brain interstitial fluid concentration of quinolones.

The side effect of quinolone antimicrobial agents (quinolones) on the CNS such as confusion, hallucinations, anxiety, agitation, depression and convulsive seizures is one of the most serious problems associated with their use as chemotherapeutic agents (Christ, 1990). Because the interaction of quinolones with the receptor of GABA in the brain is responsible for CNS side effects (Akahane *et al*., 1989), it is important to understand the mechanism for the distribution of quinolones in brain tissue and the CSF in quantitative terms. Several investigators have reported that quinolone concentrations in brain tissue and CSF are lower than in serum after systemic administration (Ichikawa *et al*., 1992; Sato *et al*., 1988). In addition, we previously demonstrated the presence of such an active transport from the CSF to blood across the BCSFB by examining the efflux of quinolones from the CSF after intracerebroventricular administration (Ooie *et al*., 1996b) and by examining the uptake of quinolones by the isolated choroid plexus (Ooie *et al*., 1996a). We have also demonstrated that brain-to-plasma and CSF-to-plasma unbound concentration of quinolones are less than unity at steady state (Ooie *et al*., 1996c). However, no report has appeared in which the efflux transport for quinolones across the BBB has been characterized. To clarify the mechanism for the restricted distribution in the brain tissue and the CSF, one of the best ways is to apply pharmacokinetic model analysis as reported previously (Dykstra *et al*., 1993; Ogawa *et al*., 1994; Sato *et al*., 1988; Wang and Sawchuk, 1995). Considering the anatomical features of the brain tissue and the CSF, the distributed model (Collins and Dedrick, 1983; Suzuki *et al*., 1997) will provide much more information about the kinetics of drug diffusion through the brain tissue.

The present study investigated the process governing the restricted distribution of quinolones in the CNS based on the distributed model. In this study, we determined the initial

Received for publication January 6, 1997.
[1] This research was supported in part by a Grant-in-Aid for Scientific Research from the Ministry of Education, Science and Culture, Japan and the Research Fund from the Human Science Foundation.
[2] Present address: Central Research Laboratories, Kyorin Pharmaceutical Co., Ltd., Nogi-machi, Shimotsuga-gun, Tochigi 329–01, Japan.
[3] Present address: Department of Pharmaceutics, Faculty of Pharmaceutical Sciences, Tohoku University, Aoba-ku, Sendai 980–77, Japan.

ABBREVIATIONS: CNS, central nervous system; GABA, γ-aminobutyric acid; CSF, cerebrospinal fluid; ISF, interstitial fluid; BBB, blood-brain barrier; BCSFB, blood-CSF barrier; NFLX, norfloxacin; OFLX, ofloxacin; FLRX, fleroxacin; PFLX, pefloxacin; AM-1155, (±)-1-cyclopropyl-6-fluoro-1,4-dihydro-8-methoxy-7-(3-methyl-1-piperazinyl)-4-oxo-3-quinolinecarboxylic acid; SPFX, sparfloxacin; HPLC, high-performance liquid chromatography.

CNS uptake of quinolones in rats. Moreover, these data, along with previously published data [brain-to-plasma and CSF-to-plasma concentration at steady state (Ooie *et al*., 1996c) and CSF concentration profiles after intracerebroventricular administration (Ooie *et al*., 1996b)] were kinetically analyzed to establish the presence of active transport for the efflux of quinolones from the brain to blood across the BBB. To clarify the mechanism of the differential distribution of quinolones in the CNS, a comparative kinetic analysis was also performed for six quinolone analogs: NFLX, AM-1155, OFLX, FLRX, SPFX and PFLX.

Materials and Methods

Materials. All the quinolones, NFLX, AM-1155, FLRX, OFLX, SPFX and PFLX were synthesized in the Central Research Laboratories of Kyorin Pharmaceutical Co., Ltd. (Tochigi, Japan). All other chemicals were commercial products of analytical grade. Male Wistar rats weighing 250 to 300 g (Japan Laboratory Animals, Inc., Tokyo, Japan) were used throughout the experiments, which were conducted according to the guidelines provided by the Institutional Animal Care Committee (Faculty of Pharmaceutical Sciences, The University of Tokyo).

***In vivo* distribution of quinolones.** Rats were anesthetized with an i.p. dose of 1.5 g/kg ethylcarbamate, and cannulation with polyethylene tubing (PE-50) was performed into the femoral artery and vein. An i.v. bolus dose of quinolone (10 mg/kg) was administered through the femoral vein cannula. At fixed times after injection of each quinolone, arterial blood specimens were withdrawn and centrifuged to obtain serum. At 1, 3, 5 and 10 min after i.v. administration, crystal-clear CSF specimens were obtained from individual rats by cisternal puncture with a 24-gauge needle (Matsushita *et al*., 1991). Immediately after collection of the CSF, each rat was decapitated and the cerebral cortex removed.

Determination of drug concentrations. Brain tissues were homogenized with 4 volumes of 0.067 M phosphate buffer (pH 7.0). After centrifugation of tissue homogenates, supernatants were used to measure drug concentrations. The concentration of quinolones in serum, tissue homogenates and CSF was determined by the HPLC as described previously (Ooie *et al*., 1997).

Kinetic analysis of serum concentration-time profiles. With the previously reported values for the serum unbound fraction (Ooie *et al*., 1996c), the unbound serum concentration of each quinolone ($C_{p,u}$) was obtained from the *in vivo* study after i.v. administration. The area under the unbound serum concentration-time curve for time t ($AUC_{u,0\text{-}t}$) of each quinolone was estimated by the linear trapezoidal rule. The apparent influx clearance across the BBB and BCSFB ($PS_{BBB,app}$ and $PS_{CSF,app}$) were obtained from *in vivo* data by dividing the brain or the CSF concentration at 1 min by the corresponding $AUC_{u,0-1\ min}$ after i.v. administration; these were used as initial estimates for the distributed model analysis described as follows. Mean $C_{p,u}$ values obtained from 6 to 12 rats after i.v. administration of each quinolone *versus* time profiles were examined by nonlinear least squares regression analysis (Yamaoka *et al*., 1981) by the following equation:

$$C_{p,u}(t) = A \cdot e^{(-\alpha \cdot t)} + B \cdot e^{(-\beta \cdot t)} \quad (1)$$

Distributed model analysis. A distributed model (Collins and Dedrick, 1983; Suzuki *et al*., 1997) has been used to analyze quinolone distribution in the CNS. The analysis was performed according to the method described previously (Suzuki *et al*., 1997) with some modifications. A diagrammatic representation of an anatomical compartment in the brain tissue and the CSF is presented in figure 1. In estimating the brain tissue concentration-time or the CSF concentration-time profiles the following assumptions were made: 1) The brain tissue and the CSF are described by a one-dimensional slab of tissue. 2) Drug permeates through the BBB and the BCSFB in both directions, *i.e*., influx and efflux. 3) There is a constant bulk flow of the CSF. 4) Drug concentration in brain ISF at the ependymal surface is the same as that in the CSF. 5) Drug diffuses through the brain tissue according to Fick's law of diffusion. 6) Drug distributes into the intracellular fluid space in the brain. Based on this model (fig. 1), the Laplace transformed equations of total brain (C_{br}) and CSF concentration (C_{CSF}) after i.v. or intracerebroventricular administration were obtained.

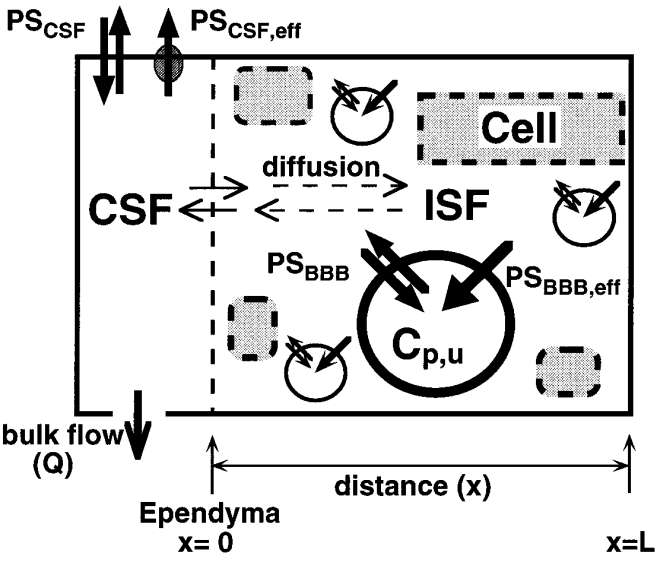

Fig. 1. Distributed model for the kinetic analysis of quinolone distribution between brain tissue, CSF and blood.

Equation 2 represents a mass balance equation describing the drug concentration in the brain tissue:

$$\frac{\partial C_{br}(x,t)}{\partial t} = D_t \cdot \frac{\partial^2 C_{br}(x,t)}{\partial x^2} + PS_{BBB} \cdot C_{p,u}(t) - \frac{(PS_{BBB} + PS_{BBB,eff})}{V_{br}} \cdot C_{br}(x,t) \quad (2)$$

where $C_{br}(x,t)$ is the drug concentration in the brain tissue at a distance, x, from the ependymal surface at time t. D_t, PS_{BBB} and $PS_{BBB,eff}$ represent the apparent diffusion coefficient through the brain tissue, the permeability clearance of symmetrical transport across the BBB and the permeability clearance of the active efflux process from the brain ISF to circulating blood across the BBB, respectively. $C_{p,u}(t)$ is the unbound drug concentration in the serum at time t, V_{br} is the distribution volume in the brain tissue defined as the concentration ratio of total brain-to-ISF.

Equation 3 represents a mass balance equation describing the drug concentration in the CSF:

$$V_{CSF} \cdot \frac{dC_{CSF}(t)}{dt} = PS_{CSF} \cdot C_{p,u}(t) - (Q + PS_{CSF} + PS_{CSF,eff}) \cdot C_{CSF}(t) + D_t \cdot Ar \cdot \frac{\partial C_{br}(0,t)}{\partial x} \quad (3)$$

where $C_{CSF}(t)$ is the drug concentration in the CSF at time t, V_{CSF} is volume of the CSF, PS_{CSF} is the symmetrical permeability clearance across the BCSFB, $PS_{CSF,eff}$ is the active efflux clearance across the

BCSFB, Q is the bulk flow rate of the CSF and Ar is the surface area of the cerebroventricular ependyma. Assuming that the ISF concentration (C_{ISF}) at the ependymal surface is the same as the CSF concentration, *i.e.*, $C_{CSF}(t) = C_{ISF}(0,t) = C_{br}(0,t)/V_{br}$, equation 3 can be converted to equation 4 as a boundary condition of equation 2, at $x = 0$.

$$V_{CSF}\cdot\frac{\partial C_{br}(0,t)}{\partial t} = V_{br}\cdot PS_{CSF}\cdot C_{p,u}(t) - (Q + PS_{CSF} + PS_{CSF,eff}) \cdot C_{br}(0,t) + (D_t\cdot Ar\cdot V_{br})\cdot\frac{\partial C_{br}(0,t)}{\partial x} \quad (4)$$

At some distance (x^*) from the ependymal surface, CSF events no longer create a driving force for diffusion flux, so that other boundary conditions of equation 2 can be defined, at $x \geq x^*$:

$$\frac{\partial C_{br}(x^*,t)}{\partial t} = PS_{BBB}\cdot C_{p,u}(t) - \frac{(PS_{BBB} + PS_{BBB,eff})}{V_{br}}\cdot C_{br}(x^*,t) \quad (5)$$

Moreover, there is no drug in brain tissue and the CSF at time $t = 0$. Thus, we have used the following relationship as an initial condition of equations 2 to 5:

$$C_{br}(x,0) = 0 \quad (6)$$

Taking the Laplace transform of equations 2 to 5, equations 7 and 8 can be obtained for the drug concentration in brain and brain ISF, respectively, at a distance x:

$$C^{iv}_{br}(x,s) = \frac{\frac{V_{br}}{V_{CSF}}\cdot PS_{CSF}\cdot\left(\frac{A}{s+\alpha}+\frac{B}{s+\beta}\right) - \left(s + \frac{Q + PS_{CSF} + PS_{CSF,eff}}{V_{CSF}}\right)\cdot\frac{\frac{PS_{BBB}\cdot A}{s+\alpha}+\frac{PS_{BBB}\cdot B}{s+\beta}}{(PS_{BBB}+PS_{BBB,eff})/V_{br}+s}}{\left(s + \frac{Q + PS_{CSF} + PS_{CSF,eff}}{V_{CSF}}\right) + \frac{D_t\cdot Ar}{V_{CSF}}\cdot V_{br}\cdot\sqrt{\frac{(PS_{BBB}+PS_{BBB,eff})/V_{br}+s}{D_t}}} \cdot\exp\left(-x\cdot\sqrt{\frac{(PS_{BBB}+PS_{BBB,eff})/V_{br}+s}{D_t}}\right) + \frac{\frac{PS_{BBB}\cdot A}{s+\alpha}+\frac{PS_{BBB}\cdot B}{s+\beta}}{(PS_{BBB}+PS_{BBB,eff})/V_{br}+s} \quad (7)$$

and

$$C^{iv}_{ISF}(x,s) = \frac{C^{iv}_{br}(x,s)}{V_{br}} \quad (8)$$

where s is the operator of time t. In this calculation, we assumed that $C_{p,u}(t)$ is given by equation 1 and $x^* \to \infty$. Defining the thickness of cerebral cortex surrounding the CSF as L, the following equation can be derived for the average drug concentration in the brain,

$$\overline{C}_{br}(s) = \frac{-\left(s + \frac{Q + PS_{CSF} + PS_{CSF,eff}}{V_{CSF}}\right)\cdot\frac{\frac{PS_{BBB}\cdot A}{s+\alpha}+\frac{PS_{BBB}\cdot B}{s+\beta}}{(PS_{BBB}+PS_{BBB,eff})/V_{br}+s} + \frac{V_{br}}{V_{CSF}}\cdot PS_{CSF}\cdot\left(\frac{A}{s+\alpha}+\frac{B}{s+\beta}\right)}{\left(s + \frac{Q + PS_{CSF} + PS_{CSF,eff}}{V_{CSF}}\right) + \frac{D_t\cdot Ar}{V_{CSF}}\cdot V_{br}\cdot\sqrt{\frac{(PS_{BBB}+PS_{BBB,eff})/V_{br}+s}{D_t}}} \cdot\frac{\left\{1 - \exp\left(-L\cdot\sqrt{\frac{(PS_{BBB}+PS_{BBB,eff})/V_{br}+s}{D_t}}\right)\right\}}{\sqrt{\frac{(PS_{BBB}+PS_{BBB,eff})/V_{br}+s}{D_t}}} \cdot\frac{1}{L} + \frac{\frac{PS_{BBB}\cdot A}{s+\alpha}+\frac{PS_{BBB}\cdot B}{s+\beta}}{(PS_{BBB}+PS_{BBB,eff})/V_{br}+s} \quad (9)$$

Moreover, considering the condition that x is zero, *i.e.*, the CSF concentration at time t, the following equation can be obtained from equations 7 and 8;

$$C^{iv}_{CSF}(s) = \frac{\left\{\begin{array}{l} -\left(s + \frac{Q + PS_{CSF} + PS_{CSF,eff}}{V_{CSF}}\right)\cdot\frac{\frac{PS_{BBB}\cdot A}{s+\alpha}+\frac{PS_{BBB}\cdot B}{s+\beta}}{(PS_{BBB}+PS_{BBB,eff})/V_{br}+s} + \frac{V_{br}}{V_{CSF}}\cdot PS_{CSF}\cdot\left(\frac{A}{s+\alpha}+\frac{B}{s+\beta}\right) \\ \hline \left(s + \frac{Q + PS_{CSF} + PS_{CSF,eff}}{V_{CSF}}\right) + \frac{D_t\cdot Ar}{V_{CSF}}\cdot V_{br}\cdot\sqrt{\frac{(PS_{BBB}+PS_{BBB,eff})/V_{br}+s}{D_t}} \end{array}\right\} + \frac{\frac{PS_{BBB}\cdot A}{s+\alpha}+\frac{PS_{BBB}\cdot B}{s+\beta}}{\frac{(PS_{BBB}+PS_{BBB,eff})}{V_{br}}+s}}{V_{br}} \quad (10)$$

With equations 9 and 10, the area under concentration-time curve of average brain tissue and the CSF, *i.e.*, AUC^{iv}_{br} and AUC^{iv}_{CSF}, respectively, can be obtained as:

$$AUC^{iv}_{br} = \lim_{s\to 0}\overline{C}_{br}(s) = \frac{-\left(\frac{Q + PS_{CSF} + PS_{CSF,eff}}{V_{CSF}}\right)\cdot\frac{\frac{PS_{BBB}\cdot A}{\alpha}+\frac{PS_{BBB}\cdot B}{\beta}}{(PS_{BBB}+PS_{BBB,eff})/V_{br}} + \frac{V_{br}}{V_{CSF}}\cdot PS_{CSF}\cdot\left(\frac{A}{\alpha}+\frac{B}{\beta}\right)}{\left(\frac{Q + PS_{CSF} + PS_{CSF,eff}}{V_{CSF}}\right) + \frac{Ar}{V_{CSF}}\cdot\sqrt{(PS_{BBB}+PS_{BBB,eff})\cdot V_{br}\cdot D_t}} \cdot\frac{\left\{1 - \exp\left(-L\cdot\sqrt{\frac{(PS_{BBB}+PS_{BBB,eff})/V_{br}}{D_t}}\right)\right\}}{\sqrt{\frac{(PS_{BBB}+PS_{BBB,eff})/V_{br}}{D_t}}} \cdot\frac{1}{L} + \left(\frac{\frac{PS_{BBB}\cdot A}{\alpha}+\frac{PS_{BBB}\cdot B}{\beta}}{PS_{BBB}+PS_{BBB,eff}}\right)V_{br} \quad (11)$$

and

$$\mathrm{AUC}^{\mathrm{iv}}_{\mathrm{CSF}} = \lim_{s\to 0} C^{\mathrm{iv}}_{\mathrm{CSF}}(s)$$

$$= \left\{ \begin{array}{l} -\left(\dfrac{Q + \mathrm{PS}_{\mathrm{CSF}} + \mathrm{PS}_{\mathrm{CSF,eff}}}{V_{\mathrm{CSF}}}\right) \\ \cdot \dfrac{\dfrac{\mathrm{PS}_{\mathrm{BBB}}\cdot A}{\alpha} + \dfrac{\mathrm{PS}_{\mathrm{BBB}}\cdot B}{\beta}}{(\mathrm{PS}_{\mathrm{BBB}} + \mathrm{PS}_{\mathrm{BBB,eff}})/V_{\mathrm{br}}} \\ + \dfrac{V_{\mathrm{br}}}{V_{\mathrm{CSF}}}\cdot \mathrm{PS}_{\mathrm{CSF}}\cdot\left(\dfrac{A}{\alpha} + \dfrac{B}{\beta}\right) \\ \hline \left(\dfrac{Q + \mathrm{PS}_{\mathrm{CSF}} + \mathrm{PS}_{\mathrm{CSF,eff}}}{V_{\mathrm{CSF}}}\right) + \dfrac{\mathrm{Ar}}{V_{\mathrm{CSF}}} \\ \cdot \sqrt{(\mathrm{PS}_{\mathrm{BBB}} + \mathrm{PS}_{\mathrm{BBB,eff}})\cdot D_{\mathrm{t}}\cdot V_{\mathrm{br}}} \end{array} + \dfrac{\dfrac{\mathrm{PS}_{\mathrm{BBB}}\cdot A}{\alpha} + \dfrac{\mathrm{PS}_{\mathrm{BBB}}\cdot B}{\beta}}{(\mathrm{PS}_{\mathrm{BBB}} + \mathrm{PS}_{\mathrm{BBB,eff}})/V_{\mathrm{br}}} \right\} / V_{\mathrm{br}} \quad (12)$$

With use of equations 11 and 12, the brain-to-unbound serum concentration ratio ($K_{\mathrm{p,u,br}}$) at steady state and the CSF-to-unbound serum concentration ratio ($K_{\mathrm{p,u,CSF}}$) at steady state can be obtained as the ratio of $\mathrm{AUC}^{\mathrm{iv}}_{\mathrm{br}}$ to the area under the unbound serum concentration-time curve ($\mathrm{AUC_u}$) and that of $\mathrm{AUC}^{\mathrm{iv}}_{\mathrm{CSF}}$ to $\mathrm{AUC_u}$ by the following equations:

$$K_{\mathrm{p,u,br}}(\text{at steady state}) = \frac{\mathrm{AUC}^{\mathrm{iv}}_{\mathrm{br}}}{\mathrm{AUC_u}}$$

$$= \frac{V_{\mathrm{br}}\cdot\left\{\mathrm{PS}_{\mathrm{CSF}} - \dfrac{\mathrm{PS}_{\mathrm{BBB}}\cdot(Q + \mathrm{PS}_{\mathrm{CSF}} + \mathrm{PS}_{\mathrm{CSF,eff}})}{(\mathrm{PS}_{\mathrm{BBB}} + \mathrm{PS}_{\mathrm{BBB,eff}})}\right\}}{L\{(Q + \mathrm{PS}_{\mathrm{CSF}} + \mathrm{PS}_{\mathrm{CSF,eff}}) \cdot \sqrt{\dfrac{(\mathrm{PS}_{\mathrm{BBB}} + \mathrm{PS}_{\mathrm{BBB,eff}})/V_{\mathrm{br}}}{D_{\mathrm{t}}}} + (\mathrm{PS}_{\mathrm{BBB}} + \mathrm{PS}_{\mathrm{BBB,eff}})\cdot \mathrm{Ar}\}} \quad (13)$$

$$\cdot\left\{1 - \exp\left(-L\cdot\sqrt{\frac{(\mathrm{PS}_{\mathrm{BBB}} + \mathrm{PS}_{\mathrm{BBB,eff}})/V_{\mathrm{br}}}{D_{\mathrm{t}}}}\right)\right\} + \frac{\mathrm{PS}_{\mathrm{BBB}}\cdot V_{\mathrm{br}}}{(\mathrm{PS}_{\mathrm{BBB}} + \mathrm{PS}_{\mathrm{BBB,eff}})}$$

and

$$K_{\mathrm{p,u,CSF}}(\text{at steady state}) = \frac{\mathrm{AUC}^{\mathrm{iv}}_{\mathrm{CSF}}}{\mathrm{AUC_u}}$$

$$= \frac{\mathrm{PS}_{\mathrm{CSF}} - \dfrac{\mathrm{PS}_{\mathrm{BBB}}\cdot(Q + \mathrm{PS}_{\mathrm{CSF}} + \mathrm{PS}_{\mathrm{CSF,eff}})}{\mathrm{PS}_{\mathrm{BBB}} + \mathrm{PS}_{\mathrm{BBB,eff}}}}{(Q + \mathrm{PS}_{\mathrm{CSF}} + \mathrm{PS}_{\mathrm{CSF,eff}}) + \mathrm{Ar}\cdot\sqrt{(\mathrm{PS}_{\mathrm{BBB}} + \mathrm{PS}_{\mathrm{BBB,eff}})\cdot D_{\mathrm{t}}\cdot V_{\mathrm{br}}}} \quad (14)$$

$$+ \frac{\mathrm{PS}_{\mathrm{BBB}}}{\mathrm{PS}_{\mathrm{BBB}} + \mathrm{PS}_{\mathrm{BBB,eff}}}$$

For an intracerebroventricular administration, mass balance equations describing the drug concentration in the brain tissue and the CSF can be obtained as equations 15 and 16, respectively.

$$\frac{\partial C_{\mathrm{br}}(x,t)}{\partial t} = D_{\mathrm{t}}\cdot\frac{\partial^2 C_{\mathrm{br}}(x,t)}{\partial x^2} - \frac{(\mathrm{PS}_{\mathrm{BBB}} + \mathrm{PS}_{\mathrm{BBB,eff}})}{V_{\mathrm{br}}}\cdot C_{\mathrm{br}}(x,t) \quad (15)$$

$$V_{\mathrm{CSF}}\cdot\frac{\mathrm{d}C_{\mathrm{CSF}}(t)}{\mathrm{d}t} = D_{\mathrm{t}}\cdot\mathrm{Ar}\cdot\frac{\partial C_{\mathrm{br}}(0,t)}{\partial x} - (Q + \mathrm{PS}_{\mathrm{CSF}} + \mathrm{PS}_{\mathrm{CSF,eff}})\cdot \mathrm{C}_{\mathrm{CSF}}(t) \quad (16)$$

Assuming that $C_{\mathrm{CSF}}(t) = C_{\mathrm{ISF}}(0,t) = C_{\mathrm{br}}(0,t)/V_{\mathrm{br}}$, the following equation can be obtained as a boundary condition of equation 15, at $x = 0$:

$$V_{\mathrm{CSF}}\cdot\frac{\partial C_{\mathrm{br}}(0,t)}{\partial t} = D_{\mathrm{t}}\cdot\mathrm{Ar}\cdot V_{\mathrm{br}}\cdot\frac{\partial C_{\mathrm{br}}(0,t)}{\partial x} - (Q + \mathrm{PS}_{\mathrm{CSF}} + \mathrm{PS}_{\mathrm{CSF,eff}})\cdot C_{\mathrm{br}}(0,t) \quad (17)$$

With the boundary condition that a distance x is significantly greater than x^*, the following relation is obtained, at $x \geq x^*$.

$$C_{\mathrm{br}}(x^*,t) = 0 \quad (18)$$

As an initial condition of equation 15, the following relationship is obtained for the CSF concentration at time zero:

$$C_{\mathrm{CSF}}(0) = \frac{\mathrm{DOSE}}{V_{\mathrm{CSF}}} \quad (19)$$

Taking the Laplace transform of equations 15 to 17, the following equations can be obtained.

$$C^{\mathrm{icv}}_{\mathrm{ISF}}(x,s) = \frac{\mathrm{DOSE}/V_{\mathrm{CSF}}}{\left(s + \dfrac{Q + \mathrm{PS}_{\mathrm{CSF}} + \mathrm{PS}_{\mathrm{CSF,eff}}}{V_{\mathrm{CSF}}}\right) + \dfrac{\mathrm{Ar}\cdot V_{\mathrm{br}}\cdot D_{\mathrm{t}}}{V_{\mathrm{CSF}}}\cdot\sqrt{\dfrac{(\mathrm{PS}_{\mathrm{BBB}} + \mathrm{PS}_{\mathrm{BBB,eff}})/V_{\mathrm{br}} + s}{D_{\mathrm{t}}}}} \cdot\exp\left(-x\cdot\sqrt{\frac{(\mathrm{PS}_{\mathrm{BBB}} + \mathrm{PS}_{\mathrm{BBB,eff}})/V_{\mathrm{br}} + s}{D_{\mathrm{t}}}}\right) \quad (20)$$

and

$$C^{\mathrm{icv}}_{\mathrm{CSF}}(s) = \frac{\mathrm{DOSE}/V_{\mathrm{CSF}}}{\left(s + \dfrac{Q + \mathrm{PS}_{\mathrm{CSF}} + \mathrm{PS}_{\mathrm{CSF,eff}}}{V_{\mathrm{CSF}}}\right) + \dfrac{\mathrm{Ar}\cdot V_{\mathrm{br}}\cdot D_{\mathrm{t}}}{V_{\mathrm{CSF}}}\cdot\sqrt{\dfrac{(\mathrm{PS}_{\mathrm{BBB}} + \mathrm{PS}_{\mathrm{BBB,eff}})/V_{\mathrm{br}} + s}{D_{\mathrm{t}}}}} \quad (21)$$

With use of equation 21, the area under concentration-time curve of the CSF after an intracerebroventricular administration ($\mathrm{AUC}^{\mathrm{icv}}_{\mathrm{CSF}}$) was obtained as:

$$\mathrm{AUC}^{\mathrm{icv}}_{\mathrm{CSF}} = \lim_{s\to 0} C^{\mathrm{icv}}_{\mathrm{CSF}}(s) = \frac{\mathrm{DOSE}}{(Q + \mathrm{PS}_{\mathrm{CSF}} + \mathrm{PS}_{\mathrm{CSF,eff}}) + \sqrt{\mathrm{Ar}^2\cdot V_{\mathrm{br}}\cdot(\mathrm{PS}_{\mathrm{BBB}} + \mathrm{PS}_{\mathrm{BBB,eff}})\cdot D_{\mathrm{t}}}} \quad (22)$$

Accordingly, the efflux clearance from the CSF after an intracerebroventricular bolus administration ($\mathrm{CL_{CSF}}$) is described by the following equation.

$$\mathrm{CL_{CSF}} = (Q + \mathrm{PS}_{\mathrm{CSF}} + \mathrm{PS}_{\mathrm{CSF,eff}}) + \sqrt{\mathrm{Ar}^2\cdot V_{\mathrm{br}}\cdot(\mathrm{PS}_{\mathrm{BBB}} + \mathrm{PS}_{\mathrm{BBB,eff}})\cdot D_{\mathrm{t}}} \quad (23)$$

Estimation of BBB and BCSFB permeability. For the model analysis, the fixed parameters were obtained in the following way. Regarding D_{t} of quinolones, the diffusion coefficient of quinolones in agar (D_{w}), was estimated from a previous report based on the molecular weight (Fenstermacher and Kaye, 1988). Based on the previously reported relationship (Fenstermacher and Kaye, 1988) between the ratio of D_{t} to D_{w} and V_{br}, defined as the ratio of the C_{br} and C_{ISF}, the D_{t} value of each quinolone was estimated and is listed in table 1. The V_{br} values of NFLX, OFLX, FLRX and PFLX were taken from a previous report which was determined by using a brain microdialysis (Ooie *et al.*, 1997). For AM-1155 and SPFX, the V_{br} value was estimated from the mean V_{br} value of NFLX, OFLX, FLRX and PFLX, *i.e.*, 1.94 ± 0.36 ml/g brain (mean ± S.E.). $\mathrm{PS_{CSF,eff}}$ was obtained from the uptake study using the isolated choroid plexus

TABLE 1
Physicochemical and pharmacokinetic parameters of quinolone antibiotics

Parameters	Units	NFLX	AM-1155	OFLX	FLRX	SPFX	PFLX
Mw[a]	–	319	375	361	369	392	333
log P_{app}[b,c]	–	−1.34	−1.14	−0.62	−0.76	−0.31	0.06
f_u[c,d]	–	0.70 ± 0.03	0.68 ± 0.03	0.77 ± 0.04	0.53 ± 0.02	0.50 ± 0.05	0.57 ± 0.03
D_w[e]	cm^2/min	4.59×10^{-4}	4.37×10^{-4}	4.42×10^{-4}	4.39×10^{-4}	4.31×10^{-4}	4.53×10^{-4}
D_t[f]	cm^2/min	5.34×10^{-5}	4.03×10^{-5}	4.08×10^{-5}	3.74×10^{-5}	3.98×10^{-5}	4.08×10^{-5}
V_{br}[g]	ml/g brain	0.975	1.94[h]	1.94	2.72	1.94[h]	2.13
A[i]	μg/ml	41.0	57.3	46.3	79.4	63.0	45.6
B[i]	μg/ml	9.05	7.22	4.70	9.67	4.76	8.33
α[i]	min^{-1}	0.980	2.90	3.39	4.25	5.59	4.10
β[i]	min^{-1}	0.0633	0.0545	0.0303	0.0676	0.0497	0.0754
$PS_{BBB,app}$[d,j]	μl/min/g brain	1.75 ± 0.76	4.38 ± 2.65	3.38 ± 0.83	17.8 ± 5.2	49.1 ± 6.1	61.8 ± 18.8
$PS_{CSF,app}$[d,k]	μl/min	1.23 ± 0.49	5.15 ± 0.97	5.98 ± 1.17	14.2 ± 3.6	33.0 ± 4.4	27.6 ± 4.3
$PS_{CSF,eff}$[l]	μl/min	0.243	1.05	3.05	2.17	2.73	4.81
CL_{CSF}[m]	μl/min	13.6 ± 3.6	22.3 ± 2.2	19.5 ± 2.2	20.5 ± 2.4	46.6 ± 8.1	34.5 ± 3.5
$K_{p,u,br}$[c,d,n]	ml/g brain	0.0111 ± 0.0066	0.106 ± 0.014	0.173 ± 0.012	0.288 ± 0.057	0.238 ± 0.023	0.254 ± 0.026
$K_{p,u,CSF}$[c,d]	–	0.0475 ± 0.005	0.134 ± 0.001	0.199 ± 0.011	0.378 ± 0.019	0.282 ± 0.027	0.355 ± 0.009

[a] Molecular weight.
[b] Apparent partition coefficient between 1-octanol and pH 7.4 buffer.
[c] Obtained from a previous report (Ooie *et al*., 1996c).
[d] Values represent the means ± S.E.
[e] Estimated from the Mw using the relationship reported previously (Fenstermacher and Kaye, 1988).
[f] Estimated from D_w using the V_{br} value based on a previous report (Fenstermacher and Kaye, 1988).
[g] Values, except for AM-1155 and SPFX, were obtained from a previous report (Ooie *et al*., 1997).
[h] Obtained from the mean value of NFLX, OFLX, FLRX and PFLX reported previously (Ooie *et al*., 1997).
[i] Obtained from the observed values in figure 2A by nonlinear least squares regression analysis by equation: $C_{p,u}(t) = A \cdot e^{(-\alpha \cdot t)} + B \cdot e^{(-\beta \cdot t)}$.
[j] Apparent BBB permeability clearance was obtained from the C_{br}/AUC_u 1 min after i.v. bolus administration.
[k] Apparent BCSFB permeability clearance was obtained from the C_{CSF}/AUC_u 1 min after i.v. bolus administration.
[l] Obtained from a previous report (Ooie *et al*., 1996a).
[m] Estimated from the CSF concentration-time profile reported previously (Ooie *et al*., 1996b) by nonlinear least squares regression analysis. Values are expressed as the mean ± calculated S.D.
[n] Obtained from reported value by subtracting the vascular volume of brain capillary lumen.

reported previously (Ooie *et al*., 1996c). The serum unbound fraction (f_u) of quinolones, Q, V_{CSF}, Ar, and L were taken from previous reports (Cserr and Dyke 1971; Ogawa *et al*., 1994; Ooie *et al*., 1996c; Suzuki *et al*., 1985) and are listed in tables 1 and 2. The total brain concentration-to-unbound serum concentration ratio ($K_{p,u,br}$) at steady state and the CSF-to-unbound serum concentration ratio ($K_{p,u,CSF}$) at steady state after i.v. constant infusion, and CL_{CSF} were taken from previous reports (Ooie *et al*., 1996b,c) and are listed in table 1.

By use of equations 9, 10 and 21, PS_{BBB}, $PS_{BBB,eff}$ and PS_{CSF} were determined simultaneously by a nonlinear least squares regression analysis program combined with the fast inverse Laplace transform algorithm (MULTI(FILT)) developed previously (Yano *et al*., 1989). For the model fitting, the following *in vivo* data were used simultaneously: 1) C_{br}-time profile after i.v. bolus administration (data shown in fig. 2B as an integration plot); 2) C_{CSF}-time profile after i.v. bolus administration (data shown in fig. 2C as an integration plot); 3) The value of $K_{p,u,br}$ at steady state after a constant i.v. infusion (table 1); 4) The value of $K_{p,u,CSF}$ at steady state after constant i.v. infusion (table 1); 5) C_{CSF}-time profile after intracerebroventricular bolus administration (taken from a previous study; Ooie *et al*., 1996b). $C_{p,u}$-time profiles of quinolones descried above were substituted for A, B, α and β in equations 9 and 10. The initial values of PS_{BBB} and PS_{CSF} were set as the apparent influx clearance obtained in *in vivo* experiment, $PS_{BBB,app}$ and $PS_{CSF,app}$, respectively. The initial value of $PS_{BBB,eff}$ was assumed to be zero. The PS_{BBB} and PS_{CSF} were allowed to vary within a range of ±50% of its initial value.

The concentration of quinolone in brain tissue was determined by subtracting the quinolone concentration in the brain vascular space from the observed total brain concentration. The blood vascular volume was assumed to be 0.020 ml/g from the reported plasma vascular volume (0.011 ml/g; Pardridge *et al*., 1991) using a hematocrit of 0.45. This value has been reported as the distribution space of mouse immunoglobulin G in rat brain (Pardridge *et al*., 1991). Reed and Woodbury (1963) obtained a value of 0.01 ml/g for the distribution of [^{14}C]inulin (5,000 Da) in rat brain, whereas they obtained value of 0.005 ml/g for [^{131}I]serum albumin (69,000 Da). With use of sucrose, Smith *et al*. (1988) also reported that the vascular space in rat brain is approximately 0.007 ml/g brain. Because we did not measure the cerebral vascular space in each rat, variations in this value may affect the analysis, in particular for quinolones (such as NFLX) whose brain distribution is limited.

Simulation of drug concentration in the CNS. The equations for $K_{p,u,br}$ (equation 13) and $K_{p,u,CSF}$ (equation 14) at steady state after i.v. administration and for CL_{CSF} after intracerebroventricular administration (equation 23) were used in the simulation study. To predict the C_{ISF} in various regions of the CNS, equations 8 and 20 were used. Unbound serum concentration *versus* time profiles of three different quinolones (NFLX, FLRX and PFLX) were taken from previous reports (Ichikawa *et al*., 1992; Jaehde *et al*., 1992; Kusajima *et al.,* 1986) and were used for the estimation of C_{ISF} after i.v. bolus administration at a dose of 10 mg/kg. Furthermore, C_{ISF} after intracerebroventricular administration at a dose of 10 μg/animal was predicted with equation 20. For the simulation study, Laplace transformed equations (equations 8 and 20) were analyzed using the fast inverse Laplace transform program (FILT; Yano *et al*., 1989).

Data analysis. Model calculation and fitting were carried out on an IBM RISC System/6000 work station using AIX XL FORTRAN Compiler/6000. The results of kinetic analysis are expressed as means ± calculated S.D. except when noted otherwise. Statistical analysis was performed by Student's t-test. Correlation was tested by Pearson's product moment correlation coefficient (r).

Results

CNS distribution of quinolones after i.v. bolus administration. The concentrations in the serum, brain tissue and the CSF were determined after i.v. administration of 10 mg/kg of each quinolone. By using the previously reported f_u for each quinolone (table 1; Ooie *et al*., 1996c), the $C_{p,u}$-time profiles were obtained and are shown in figure 2A. The phar-

macokinetic parameters to describe the curve were obtained by nonlinear least squares regression analysis and are listed in table 1. Figure 2B illustrates initial uptake of quinolones into the CNS after i.v. administration as an integration plot ($K_{p,u,br}$ *vs.* $AUC_u/Cp,u$; Patlak *et al.,* 1983). In principle, extrapolation of the $K_{p,u,br}$ *versus* $AUC_u/C_{p,u}$ line yields the cerebral vascular volume as the *y*-intercept. As shown in figure 2B, however, the values of the *y*-intercept for some quinolones are much higher than the vascular space; *e.g.*, 0.13 and 0.14 ml/g brain for SPFX and PFLX, respectively. These results may be accounted for by considering the rapid passage of these two quinolones across the BBB. To quantify this rapid passage by model analysis, the $PS_{BBB,app}$ value was determined with the early time point (1 min after i.v. administration) data, rather than the slope of the integration plot, assuming no adsorption of quinolone to the luminal surface of brain capillaries and no back flux from the brain into the circulating blood. The $PS_{BBB,app}$ values for six kinds of quinolone antibiotics (table 1) were further used as the initial value for PS_{BBB} in the kinetic analysis. Comparing the values of $PS_{BBB,app}$, NFLX and PFLX were the smallest and greatest, respectively, and a 35-fold difference was observed between them. Figure 2C illustrates the $K_{p,u,CSF}$ *versus* AUC $_u$ /$C_{p,u}$ plot. Similarly, $PS_{CSF,app}$ values were determined and are listed in table 1. Comparing the values of $PS_{CSF,app}$, NFLX and SPFX were the smallest and greatest, respectively, and a 27-fold difference was observed between them.

Distributed model analysis. By use of equations 9, 10 and 21, PS_{BBB}, $PS_{BBB,eff}$ and PS_{CSF} were obtained by nonlinear least squares regression analysis. Figure 3 represents the comparison between observed and fitted values for the six quinolones. As shown in figure 3, A, C, D and E, a fairly good coincidence was observed between observed and model-fitted values for the brain concentration after i.v. bolus administration, the steady state $K_{p,u,br}$ and $K_{p,u,CSF}$ after i.v. constant infusion and the CSF concentration after intracerebroventricular bolus administration. For the CSF concentration after i.v. bolus administration, the model values were relatively smaller than the observed values (fig. 3B).

The fitted parameters for the quinolones (PS_{BBB}, $PS_{BBB,eff}$ and PS_{CSF}) are summarized in table 3. The PS_{BBB} values of SPFX and PFLX were about 80-fold greater than the PS_{BBB} value of NFLX. Moreover, the $PS_{BBB,eff}$ value was 11- to 260-fold greater than the PS_{BBB} value (table 3). With use of the fitted parameters obtained, the net flux across the BBB [$PS_{BBB}/(PS_{BBB} + PS_{BBB,eff})$] was also calculated. A good correlation was observed ($r = 0.93$, $P < .01$) between net flux (table 3) and steady state $K_{p,br}$ values (table 1). PS_{CSF} of NFLX was smaller than Q, whereas the PS_{CSF} of SPFX was 5-fold greater than Q (table 3). Assuming that $PS_{BBB,eff}$ equals zero, the $K_{p,u,br}$ values were simulated to be approximately 5- to 10-fold greater than the observed values (data not shown).

TABLE 2

Physiological and anatomical parameters used for the distributed model analysis

Parameters	Units	Values
Q	μl/min	2.9[a]
Ar	cm^2	2.0[b]
V_{CSF}	μl	250[c]
L	mm	2.0[b]

[a] Taken from reported values (Suzuki *et al*., 1985).
[b] Taken from reported values (Ogawa *et al*., 1994).
[c] Taken from reported values (Cserr and Dyke, 1971).

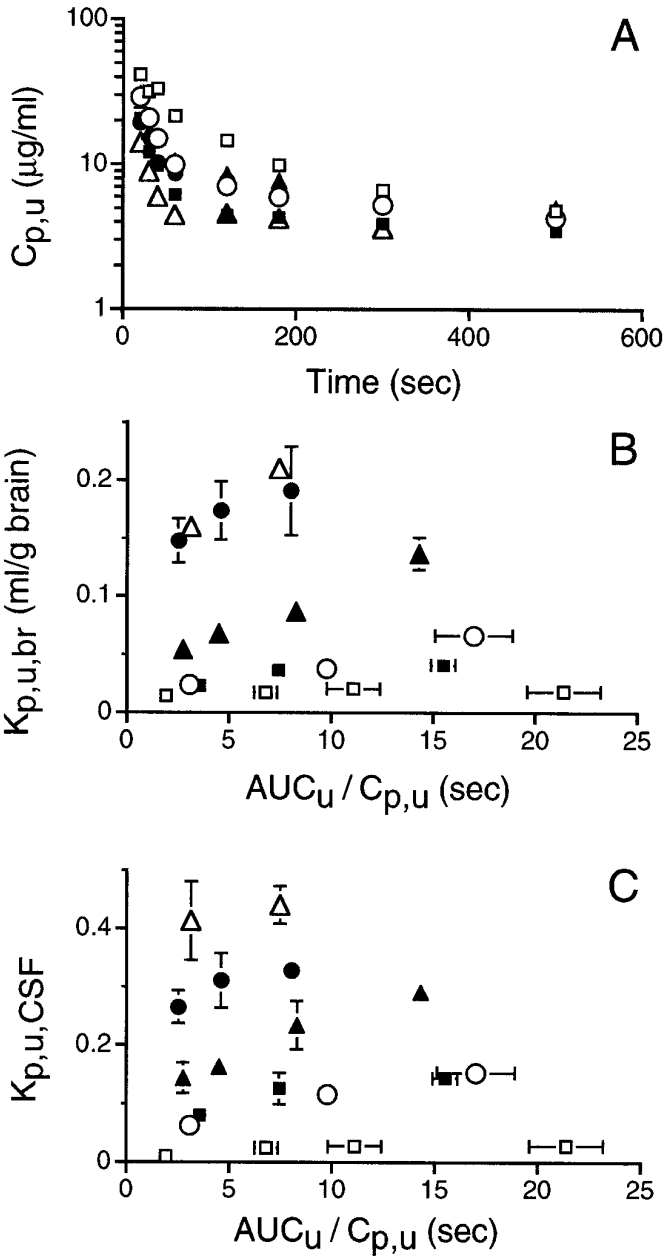

Fig. 2. Unbound serum concentration-time profile (A), total brain-to-unbound serum concentration ratio ($K_{p,u,br}$; B) *versus* the ratio of the area under the unbound serum concentration time curve (AUC_u) to the unbound serum concentration ($C_{p,u}$), and CSF-to-unbound serum concentration ratio ($K_{p,u,CSF}$; C) *versus* the ratio of the area under the unbound serum concentration time curve (AUC_u) to the unbound serum concentration ($C_{p,u}$) of quinolones in rats. Six different quinolones (10 mg/kg) were administered intravenously and blood samples were collected. At 1, 3, 5 and 10 min after dosing, CSF was obtained from individual rats by cisternal puncture. Immediately after the collection of CSF, the cerebrum was removed. Each point represents the mean ± S.E. of 4 to 12 animals. Where error bars are not shown, the S.E. is contained within the symbol. □, NFLX; ○, AM-1155; ▲, FLRX; ■, OFLX; △, SPFX; ●, PFLX.

As shown in figure 4A, a fairly good correlation was observed between the PS_{BBB} and the octanol-water partition coefficient (Ooie *et al*., 1996c) for the quinolones examined ($r = 0.90$, $P < .01$). There was also a good correlation between

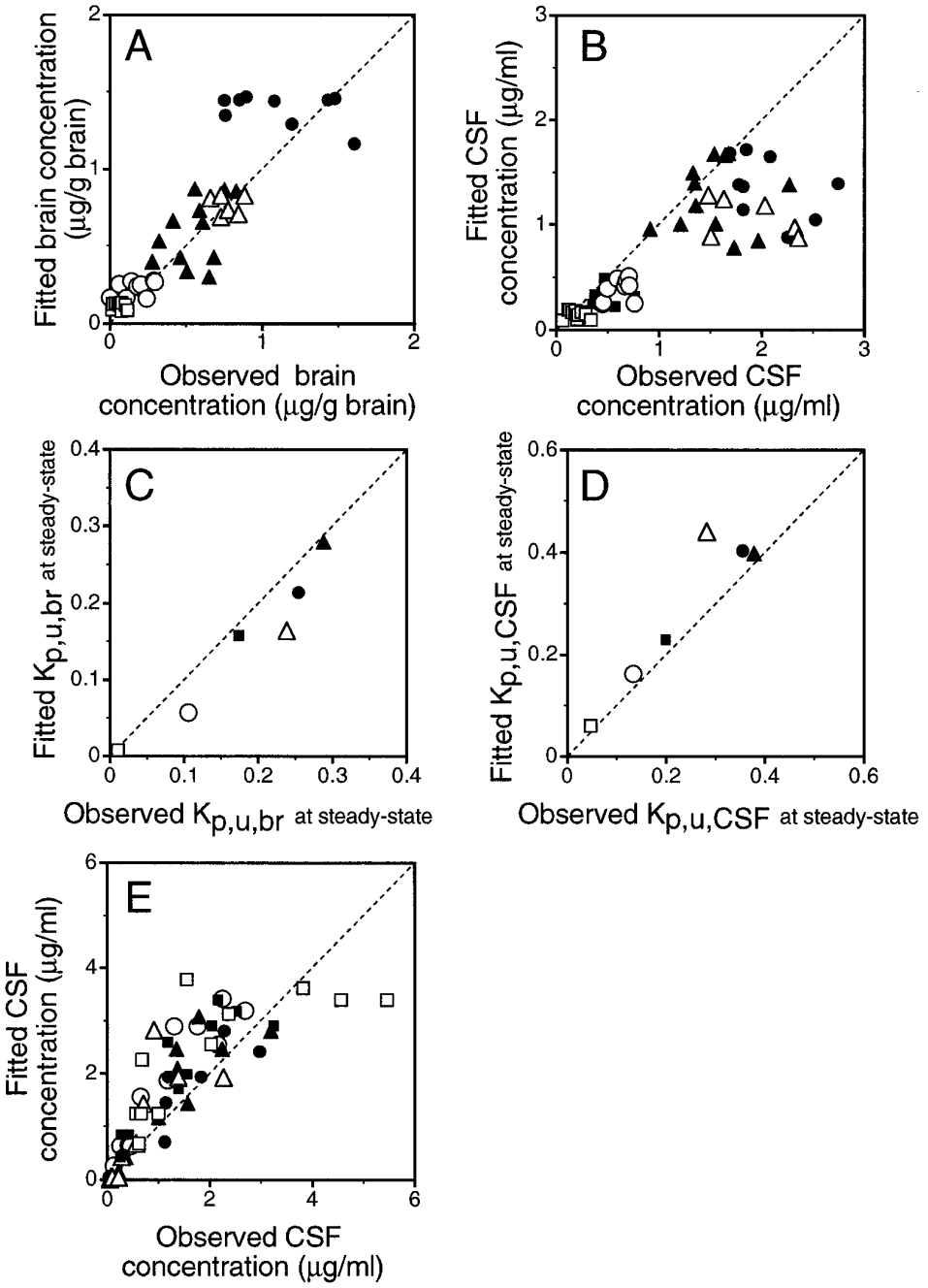

Fig. 3. Comparison of fitted and observed values for quinolone distribution in the CNS. (A) total brain concentration after i.v. bolus administration; (B) CSF concentration after i.v. bolus administration; (C) brain-to-unbound serum concentration ratio ($K_{p,u,br}$) at steady state, the observed values were taken from a previous report (Ooie *et al*., 1996c); (D) CSF-to-unbound serum concentration ratio ($K_{p,u,CSF}$) at steady state, the observed values were taken from a previous report (Ooie *et al*., 1996c); (E) CSF concentration after intracerebroventricular administration, the observed values were taken from a previous report (Ooie *et al*., 1996b). □, NFLX; ○, AM-1155; ▲, FLRX; ■, OFLX; △, SPFX; ●, PFLX.

TABLE 3

Permeability clearance of quinolones obtained by nonlinear least squares regression analysis combined with a fast inverse Laplace transform algorithm (MULTI(FILT))

Parameters	Units	NFLX	AM-1155	OFLX	FLRX	SPFX	PFLX
PS_{BBB}	μl/min/g	0.88 ± 5.00	6.57 ± 3.53	5.07 ± 3.31	11.9 ± 4.4	73.7 ± 23.7	72.6 ± 15.7
$PS_{BBB,eff}$	μl/min/g	228 ± 150	348 ± 110	85.9 ± 42.6	174 ± 47	998 ± 310	787 ± 179
PS_{CSF}	μl/min	0.62 ± 0.34	2.57 ± 0.36	2.99 ± 0.34	8.21 ± 0.81	16.5 ± 2.7	14.5 ± 1.5
$PS_{BBB}/(PS_{BBB} + PS_{BBB,eff})$		0.004 ± 0.022	0.019 ± 0.011	0.056 ± 0.045	0.064 ± 0.029	0.069 ± 0.030	0.084 ± 0.025

Each value represents the mean ± calculated S.D.

the PS_{CSF} and the octanol-water partition coefficient ($r = 0.88$, $P < .01$), but not for the $PS_{BBB,eff}$ ($r = 0.52$, not significant).

Because the penetration of ligands across the erythrocyte membrane is rapid enough (Simanjuntak *et al*., 1991), the unbound plasma concentration equals the unbound blood concentration by their definition. The kinetic parameters defined for the plasma unbound concentration, therefore, can be used if these values are defined for the unbound blood concentration.

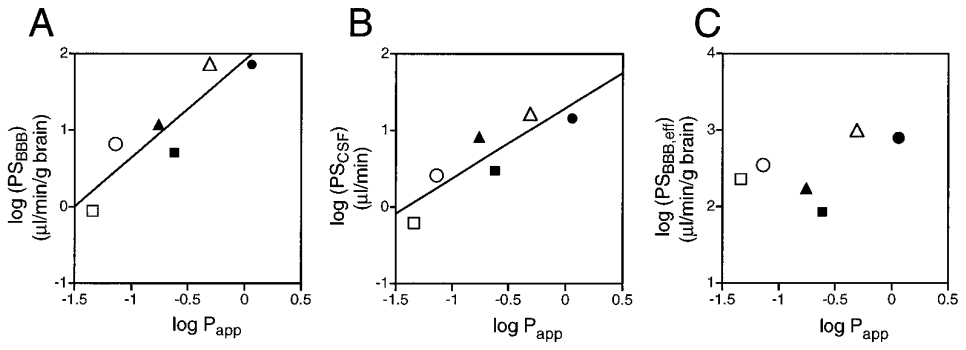

Fig. 4. Relationship between the octanol-water partition coefficient (log P_{app}) and symmetrical permeability clearance across the BBB (PS_{BBB}; A), symmetrical permeability clearance across the BCSFB (PS_{CSF}; B) and asymmetric clearance across the BBB ($PS_{BBB,eff}$; C). The straight line represents the result of linear regression analysis. □, NFLX; ○, AM-1155; ▲, FLRX; ■, OFLX; △, SPFX; ●, PFLX.

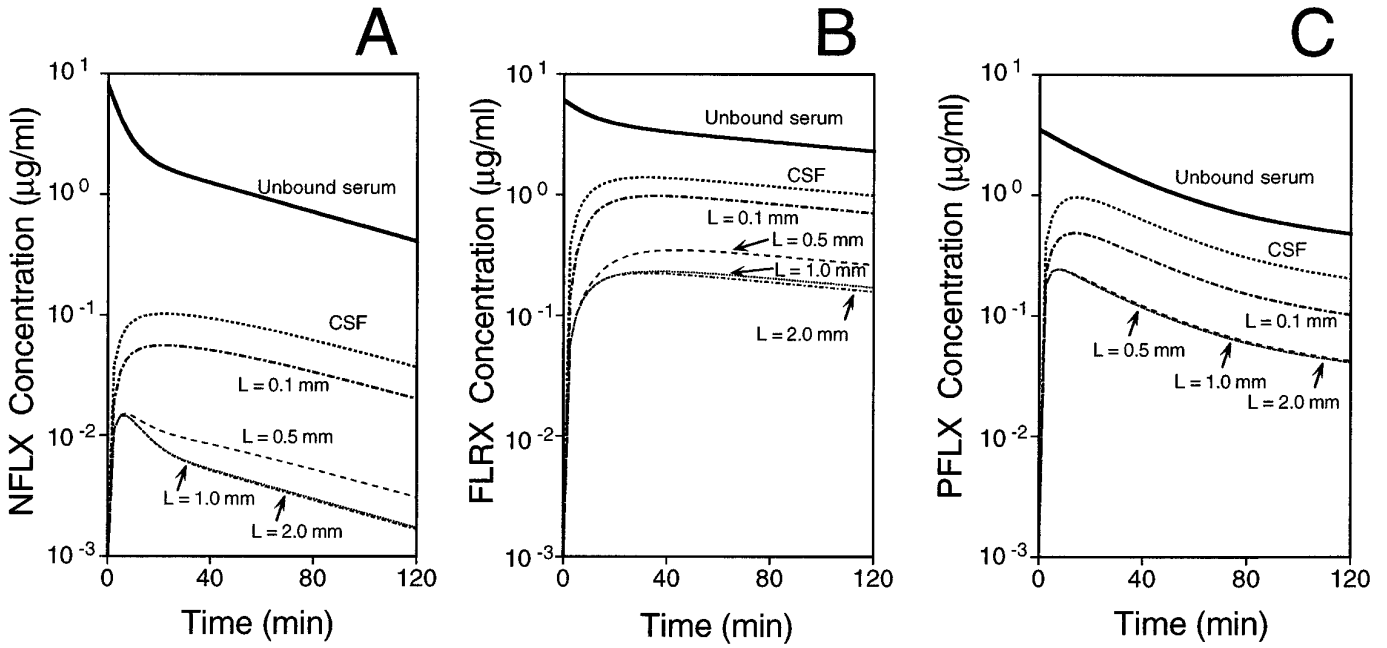

Fig. 5. Prediction of concentration-time profile of quinolone distribution in various regions of the CNS and serum after i.v. bolus administration of quinolones, 10 mg/kg, to rats. (A) NFLX; (B) FLRX; (C) PFLX. Values close to the line represent the distance from the ependymal surface.

Prediction of brain ISF concentration as a function of the distances from the ependymal surface. Figure 5 represents the C_{ISF}-time profiles as a function of the distance from the ependymal surface after i.v. bolus administration of NFLX, FLRX and PFLX at a dose of 10 mg/kg to rats. A significant gradient of C_{ISF} was observed as a function of the distance from the surface. No significant difference in C_{ISF} was observed at cerebral regions more than 1 mm distant from the ependymal surface (fig. 5).

Figure 6 represents the C_{ISF}-time profiles as a function of the distance from the ependymal surface after intracerebroventricular bolus administration of NFLX, FLRX and PFLX at a dose of 10 μg/animal to rats. During the terminal phase, an approximately 10- and 1000-fold difference was observed between the CSF and ISF concentrations at a distance of 0.5 mm and 1 mm from the surface of ependymal cell layer, respectively (fig. 6).

Effect of diffusion through brain tissue and active efflux clearance across the BCSFB on $K_{p,u,br}$ and $K_{p,u,CSF}$ at steady state. The equation representing $K_{p,u,br}$ and $K_{p,u,CSF}$ at steady state were obtained as equations 13 and 14, respectively. Assuming that the diffusion coefficient through the brain tissue is zero, the $K_{p,u,br}$ and the $K_{p,u,CSF}$ values were estimated and compared with the fitted values in figure 7, A and B, respectively. The simulated $K_{p,u,br}$ value was lower than that of the fitted value, whereas the simulated $K_{p,u,CSF}$ value was greater than the fitted value for all quinolones studied. Figures 8, A and B, represent the effect of the active efflux clearance across the BCSFB on the $K_{p,u,br}$ and the $K_{p,u,CSF}$ values, respectively. Only a slight difference was observed between the fitted and simulated values even if $PS_{CSF,eff}$ was assumed to be zero.

Analysis of the efflux clearance from the CSF after an intracerebroventricular bolus administration. The CL_{CSF} is given as a function of Q, PS_{CSF}, $PS_{CSF,eff}$, D_t and $PS_{BBB,eff}$ (equation 23). By substituting the fitted parameter values to equation 23, CL_{CSF} was calculated. As shown in figure 9, a fairly good agreement between observed and fitted values was obtained for CL_{CSF}. Figure 9 also indicates that the diffusion through the brain tissue and the subsequent efflux across the BBB plays an important role in the elimination of quinolones from the CSF after intracerebroventricular administration.

Discussion

The drug concentration in the brain ISF is a determinant for *in vivo* CNS effects, although several processes needed to

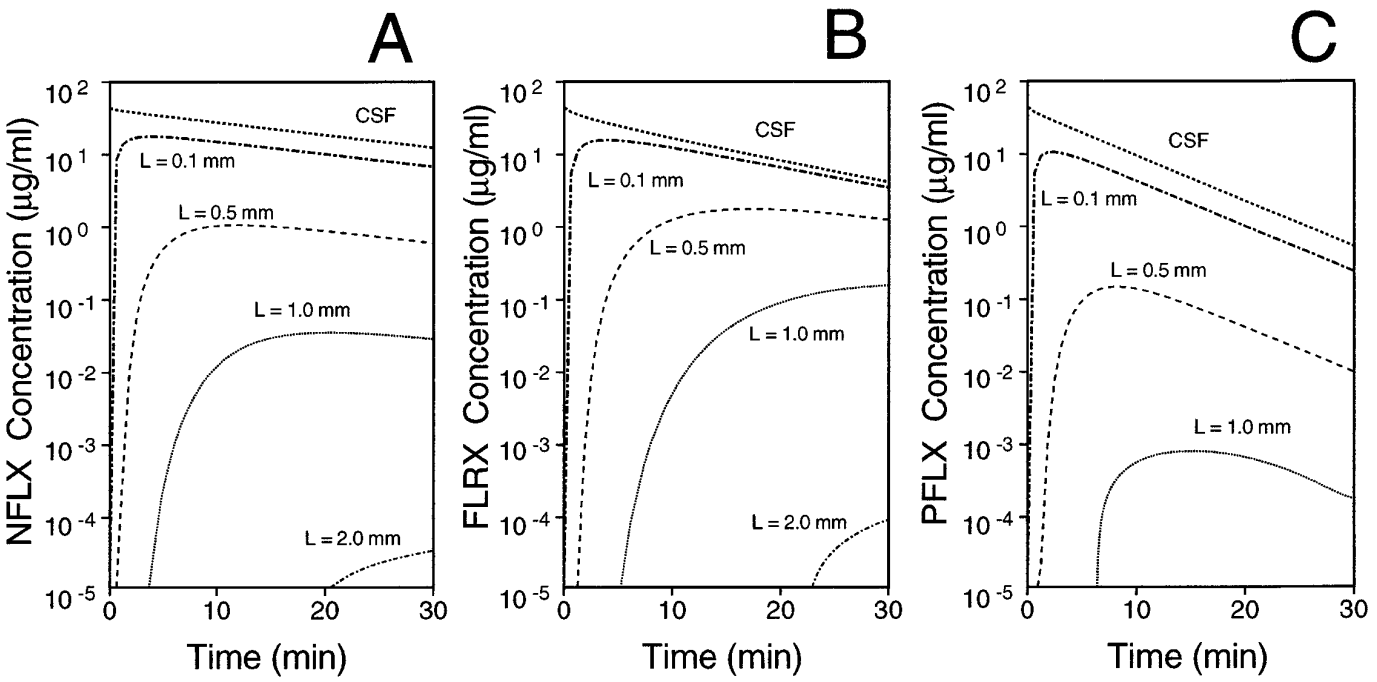

Fig. 6. Prediction of brain ISF concentration-time profiles in various regions of the CNS after intracerebroventricular administration of quinolones, 10 μg/animal, to rats. (A) NFLX; (B) FLRX; (C) PFLX. Values close to the line represent the distance from the ependymal surface.

be considered for the precise analysis. Because there is free ligand exchange between CSF and ISF, the distributed model should be suitable for the kinetic analysis of drug distribution in the brain tissue and CSF (Collins and Dedrick, 1983; Suzuki *et al*., 1997). The major assumptions of this model are that there is free ligand exchange between CSF and ISF, and that the ligand molecules diffuse through the brain parenchyma according to Fick's law. Both these assumptions have been confirmed as being justified by previous reports in which the ligand concentration in the brain parenchyma was determined as a function of the distance from the ependymal surface in the ventriculocisternal perfusion experiments. The kinetic analysis of the experimental data revealed that the CNS profiles can be described by the assumptions described previously (Patlak and Fenstermacher, 1975; Blasberg *et al*., 1975; Fenstermacher and Davson, 1982). In addition, Dykstra and his collaborators (1993) confirmed this hypothesis by examining the brain concentration profiles after ligand administration through a microdialysis probe implanted into the cerebral cortex. Fenstermacher and Kaye (1988) summarized the D_t values determined by the method described previously and found a good relationship between D_t and D_w. Based on this relationship, we estimate the D_t values for quinolone antibiotics.

The efflux clearance across the BBB (the sum of PS_{BBB} and $PS_{BBB,eff}$) was 12- to 260-fold greater than PS_{BBB}. Moreover, after i.v. bolus administration, the concentration gradient was observed from CSF to brain ISF; the brain acts as a sink (fig. 5). These results provide kinetic evidence to support the hypothesis that a significant efflux transport from the brain ISF to the capillary lumen across the BBB is the predominant factor involved in the restricted distribution of quinolones in brain ISF after systemic administration (Ooie *et al*., 1997). Furthermore, the good correlation between $PS_{BBB}/(PS_{BBB} + PS_{BBB,eff})$ and the $K_{p,u,br}$ at the steady state indicated that the transport across the BBB is a determinant for the different distribution of these quinolones in the brain tissue.

To evaluate the effect of drug diffusion through the brain tissue on the apparent distribution in brain tissue and the CSF, simulation studies were performed for the prediction of $K_{p,u,br}$ and $K_{p,u,CSF}$ at steady state assuming no drug diffusion through brain tissue. As shown in figure 7, 16% to 52% reduction was observed in $K_{p,u,br}$ whereas 170% to 45% increase was demonstrated in $K_{p,u,CSF}$. These results suggest that the CSF acts as a pool to supply quinolone molecules to the brain ISF by diffusion, whereas brain ISF acts as a sink to eliminate quinolone molecules from the CSF at steady state following i.v. administration.

Regarding the efflux across the BCSFB, we have previously demonstrated that the *in vitro* uptake clearance of β-lactam antibiotics by the isolated choroid plexus is similar to the *in vivo* efflux clearance across the BCSFB determined by intracerebroventricular administration (Ogawa *et al*., 1994). We have also found that quinolone is transported by the isolated choroid plexus *via* an organic anion transport system which is also responsible for the efflux of β-lactam antibiotics across the BCSFB (Ooie *et al*., 1996a). Therefore, in the present study, we have assumed that $PS_{CSF,eff}$ of quinolones is the same as the uptake clearance determined by the isolated choroid plexus reported previously (Ooie *et al*., 1996c). Assuming that the $PS_{CSF,eff}$ is zero, the participation of active efflux transport across the BCSFB was studied by examining the apparent distribution in the brain tissue and the CSF. As shown in figure 8, active efflux transport across the BCSFB plays only a minor role in the distribution of quinolones both in brain tissue and the CSF. These results are in good agreement with the results shown in figure 9 that less than 20% of the apparent efflux clearance from the CSF is caused by active efflux transport across the BCSFB. Unlike

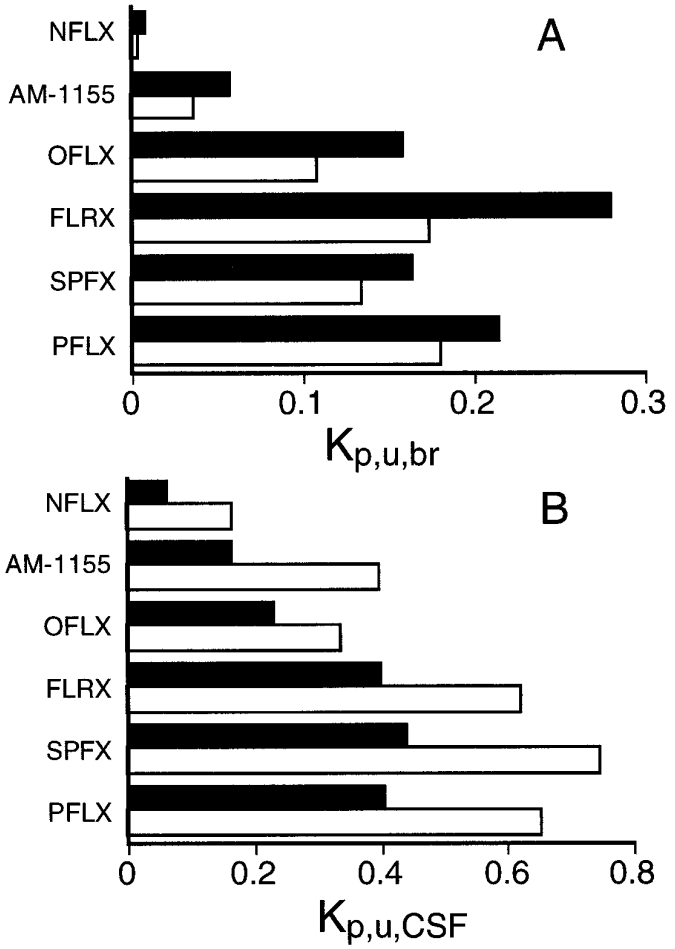

Fig. 7. Comparison between fitted (solid bars) and simulated (open bars) $K_{p,u,br}$ and $K_{p,u,CSF}$ values assuming no diffusion through brain parenchyma tissue. (A) brain-to-unbound serum concentration ratio at steady state; (B) CSF-to-unbound serum concentration ratio at steady state.

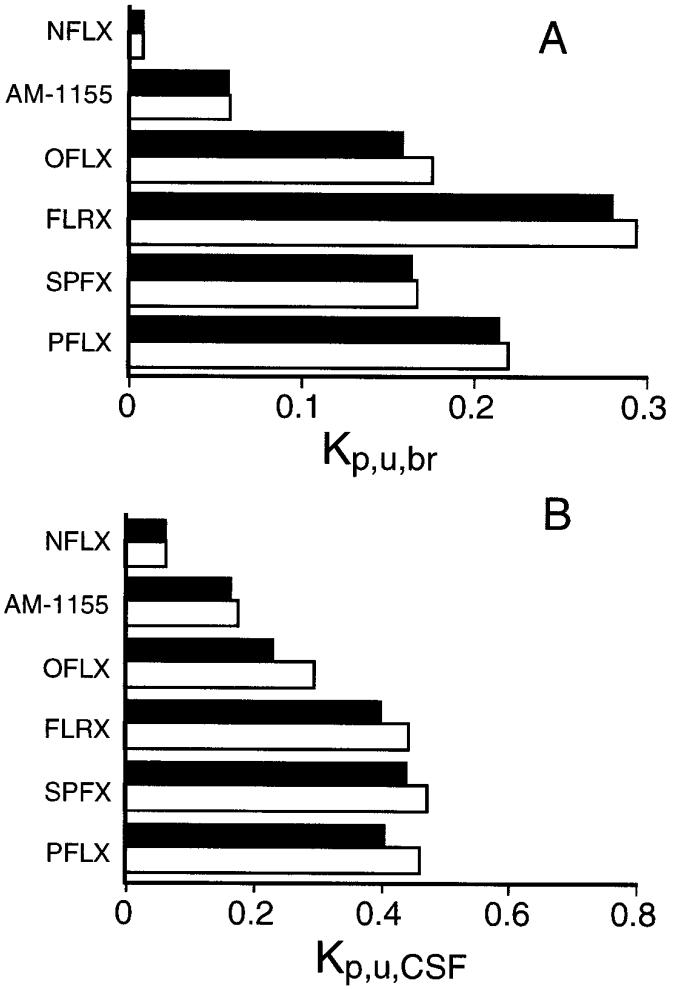

Fig. 8. Comparison between fitted (solid bars) and simulated (open bars) $K_{p,u,br}$ and $K_{p,u,CSF}$ values assuming no active efflux *via* a BCSFB ($PS_{CSF,eff} = 0$). (A) brain-to-unbound serum concentration ratio at steady state; (B) CSF-to-unbound serum concentration ratio at steady state.

β-lactam antibiotics reported previously (Ogawa *et al.,* 1994), these simulation results also agree well with our previous finding that probenecid has no significant inhibitory effect on the apparent elimination of FLRX from the CSF after intracerebroventricular administration and that the elimination of FLRX was not saturable (Ooie *et al*., 1996b).

As a barrier function of brain capillary endothelial cells, it has been reported that P-glycoprotein acts as a primary active efflux transport system to pump vincristine (Tsuji *et al*., 1992), cyclosporin A (Tatsuta *et al*., 1992) and vinblastine (Schinkel *et al*., 1994) out of the brain into the circulating blood. Moreover, several reports have provided kinetic evidence that an efflux transport system for β-lactam antibiotics (Matsushita *et al*., 1991), azidodeoxythymidine (Dykstra *et al*., 1993; Takasawa *et al*., 1997) and valproic acid (Adkison *et al*., 1994) is located on the BBB. Although this transport system has not been characterized yet, the transporter may be different from P-glycoprotein (*mdr1*).

Regarding the CNS toxicity of quinolone antibiotics, drug concentrations in the brain ISF would be a determinant for their duration and severity. The present study suggests that the affinity of quinolones to a putative carrier-mediated efflux transport system may be important in reducing brain ISF concentrations and consequent CNS effect. Although a 10-fold difference was observed between SPFX and OFLX for $PS_{BBB,eff}$ (table 3), comparison with the physicochemical nature of quinolones revealed that there is no significant relationship between the lipophilicity and $PS_{BBB,eff}$ (fig. 4C). Because it has not been possible to demonstrate the efflux transport of quinolones in the primary cultured bovine brain capillary endothelial cells (Jaehde *et al*., 1993), presumably because of the down-regulation of the expression of the transporter, it would be important to use an *in vivo* method to characterize the transport property across the BBB. One of the rational ways to characterize the efflux transport system at the BBB is to examine the elimination of ligand from the brain after microinjection into the cerebral cortex (Leininger *et al*., 1991; Banks *et al*., 1994; Kakee *et al*., 1996).

In conclusion, it has been demonstrated that the significantly limited distribution of quinolones in the brain tissue is caused by the presence of an active efflux transport system located on the BBB. Depending on the distance from the ependymal surface, there is a significant concentration gradient from the CSF to the brain ISF after systemic administration. One of the most important factors regulating brain ISF concentrations of quinolones may be an affinity for the putative efflux transport system on the BBB.

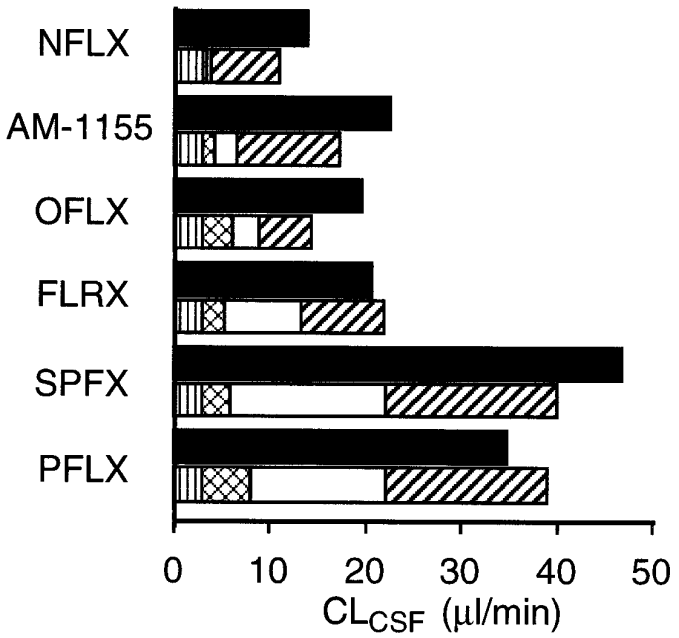

Fig. 9. Contribution of the CSF bulk flow rate (striped bars), active efflux clearance across the BCSFB (cross-hatched bars), symmetrical permeability clearance across the BCSFB (open bars) and diffusion through the brain tissues and the resultant efflux across the BBB (hatched bars) to apparent CSF efflux clearance after intracerebroventricular bolus administration. Observed values of the apparent CSF efflux clearance were taken from a previous report (Ooie *et al*., 1996b) and represented as closed bars.

References

Adkison, K. D. K., Artru, A. A., Powers, K. M. and Shen, D. D.: Contribution of probenecid-sensitive anion transport processes at the brain capillary endothelium and choroid plexus to the efficient efflux of valproic acid from the central nervous system. J. Pharmacol. Exp. Ther. **268:** 797–805, 1994.

Akahane, K., Sekiguchi, M., Une, T. and Osada, Y.: Structure-epileptogenicity relationship of quinolones with special reference to their interaction with γ-aminobutyric acid receptor sites. Antimicrob. Agents Chemother. **33:** 1704–1708, 1989.

Banks, W. A., Kastin, A. J., Sam, H. M., Cao, V. T., King, B., Maness, L. M., Schally, A. V.: Saturable efflux of the peptides RC-160 and Tyr-MIF-1 by different parts of the blood-brain barrier. Brain Res. Bull. **35:** 179–82, 1994.

Blasberg, R. G., Patlak, C. and Fenstermacher, J. D.: Intrathecal chemotherapy: Brain tissue profiles after ventriculocisternal perfusion. J. Pharmacol. Exp. Ther. **195:** 73–83, 1975.

Christ, W.: Central nervous system toxicity of quinolones: Human and animal findings. J. Antimicrob. Chemother. **26:** suppl. B, 219–225, 1990.

Collins, J. M. and Dedrick, R. L.: Distributed model for drug delivery to CSF and brain tissue. Am. J. Physiol. **245:** R303–R310, 1983.

Cserr, H. F. and Dyke, D. H.: 5-Hydroxyindoleacetic acid accumulation by isolated choroid plexus. Am. J. Physiol. **220:** 718–723, 1971.

Dykstra, K. H., Arya, A., Arriola, D. M., Bungay, P. M., Morrison, P. F. and Dedrick, R. L.: Microdialysis study of zidovudine (AZT) transport in rat brain. J. Pharmacol. Exp. Ther. **267:** 1227–1236, 1993.

Fenstermacher, J. D. and Davson, H.: Distribution of two model amino acids from cerebrospinal fluid to brain and blood. Am. J. Physiol. **242:** F171–F180, 1982.

Fenstermacher, J. and Kaye, T.: Drug "diffusion" within the brain. Ann. N.Y. Acad. Sci. **531:** 29–39, 1988.

Ichikawa, N., Naora, K., Hayashibara, M., Katagiri, Y. and Iwamoto, K.: Effect of fenbufen on the entry of new quinolones, norfloxacin and ofloxacin, into the central nervous system in rats. J. Pharm. Pharmacol. **44:** 915–920, 1992.

Jaehde, U., Langemeijer, M. W. E., De Boer, A. G. and Breimer, D. D.: Cerebrospinal fluid transport and disposition of the quinolones ciprofloxacin and pefloxacin in rats. J. Pharmacol. Exp. Ther. **263:** 1140–1146, 1992.

Jaehde, U., Goto, T., De. Boer, A. G. and Breimer, D. D.: Blood-brain barrier transport rate of quinolone antibacterials evaluated in cerebrovascular endothelial cell cultures. Eur. J. Pharm.Sci. **1:** 49–55, 1993.

Kakee, A., Terasaki, T. and Sugiyama, Y.: Brain efflux index as a novel method of analyzing efflux transport at the blood-brain barrier. J. Pharmacol. Exp. Ther. **277:** 1550–1559, 1996.

Kusajima, H., Ishikawa, N., Machida, M., Uchida, H. and Irikura. T.: Pharmacokinetics of a new quinolone, AM-833, in mice, rats, rabbits, dogs, and monkeys. Antimicrob. Agents Chemother. **30:** 304–309, 1986.

Leininger, B., Ghersi-Egea, J. F., Siest, G., Minn, A.: *In vivo* study of the elimination from rat brain of an intracerebrally formed xenobiotic metabolite, 1-naphthyl-beta-D-glucuronide. J. Neurochem. **56:** 1163–1168, 1991.

Matsushita, H., Suzuki, H., Sugiyama, Y., Sawada, Y., Iga, T., Kawaguchi, Y. and Hanano, M.: Facilitated transport of cefodizime into the rat central nervous system. J. Pharmacol. Exp. Ther. **259:** 620–625, 1991.

Ogawa, M., Suzuki, H., Sawada, Y., Hanano, M. and Sugiyama, Y.: Kinetics of active efflux *via* choroid plexus of β-lactam antibiotics from the CSF into the circulation. Am. J. Physiol. **266:** R392–R399, 1994.

Ooie, T., Suzuki, H., Terasaki, T. and Sugiyama, Y.: Characterization of the transport properties of a quinolone antibiotic, fleroxacin, in rat choroid plexus. Pharm. Res. **13:** 512–516, 1996a.

Ooie, T., Suzuki, H., Terasaki, T. and Sugiyama, Y.: Kinetics of quinolone antibiotics in rats: Efflux from cerebrospinal fluid to the circulation. Pharm. Res. **13:** 1072–1076, 1996b.

Ooie, T., Suzuki, H., Terasaki, T. and Sugiyama, Y.: Comparative distribution of quinolone antibiotics in cerebrospinal fluid and brain in rats and dogs. J. Pharmacol. Exp. Ther. **278:** 590–596, 1996c.

Ooie, T., Terasaki, T., Suzuki, H. and Sugiyama, Y.: Quantitative brain microdialysis study on the mechanism of quinolones distribution in the central nervous system. Drug. Metab. Dispos. **25:** 784–789, 1997.

Pardridge, W. M., Buciak, J. L. and Friden, P. M.: Selective transport of anti-transferrin receptor antibody through the blood-brain barrier *in vivo*. J. Pharmacol. Exp. Ther. **259:** 66–70, 1991.

Patlak, C. S. and Fenstermacher, J. D.: Measurements of dog blood-brain transfer constants by ventriculocisternal perfusion. Am. J. Physiol. **229:** 877–884, 1975.

Patlak, C. S., Blasberg, R. G. and Fenstermacher, J. D.: Graphical evaluation of blood-to-brain transfer constants from multiple-time uptake data. J. Cereb. Blood Flow Metab. **3:** 1–7, 1983.

Reed, D. J. and Woodbury, D. M.: Kinetics of movement of iodide, sucrose, inulin and radio-iodinated serum albumin in the central nervous system and cerebrospinal fluid of the rat. J. Physiol. (Lond.) **169:** 816–850, 1963.

Sato, H., Okezaki, E., Yamamoto, S., Nagata, O., Kato, H. and Tsuji, A.: Entry of the new quinolone antibacterial agents of ofloxacin and NY-198 into the central nervous system in rats. J. Pharmacobio-Dyn. **11:** 386–394, 1988.

Schinkel, A. H., Smit, J. J. M., van Tellingen, O., Beijnen, J. H., Wagenaar, E., van Deemter, L., Mol, C. A. A. M., van der Valk, M. A., Robanus-Maandag, E. C., te Riele, H. P. J., Berns, A. J. M. and Borst, P.: Disruption of the mouse *mdr1a* P-glycoprotein gene leads to a deficiency in the blood-brain barrier and to increased sensitivity to drugs. Cell **77:** 491–502, 1994.

Simanjuntak, M. T., Sato, H., Tamai, I., Terasaki, T. and Tsuji, A.: Transport of the new quinolone antibacterial agents of lomefloxacin and ofloxacin by rat erythrocytes, and its relation to the nicotinic acid transport system. J. Pharmacobio-Dyn. **14:** 475–481, 1991.

Smith, Q. R., Ziylan, Y. Z., Robinson, P. J. and Rapoport, S. I.: Kinetics and distribution volumes for tracers of different sizes in the brain plasma space. Brain Res. **462:** 1–9, 1988.

Suzuki, H., Sawada, Y., Sugiyama, Y., Iga, T. and Hanano, M.: Saturable transport of cimetidine from cerebrospinal fluid to blood in rats. J. Pharmacobio-Dyn. **8:** 73–76, l985.

Suzuki, H., Terasaki, T. and Sugiyama, Y.: Role of efflux transport across the blood-brain barrier and blood-cerebrospinal fluid barrier on the disposition of xenobiotics in the central nervous system. Adv. Drug Deliv. Rev., **25:** 257–285, 1997.

Takasawa, K., Terasaki, T., Suzuki, H. and Sugiyama, Y.: *In vivo* evidence for carrier-mediated efflux transport of 3′-azido-3′-deoxythymidine and 2′,3′-dideoxyinosine across the blood-brain barrier *via* a probenecid-sensitive transport system. J. Pharmacol. Exp. Ther. **281:** 369–375, 1997.

Tatsuta, T., Naito, M., Oh-hara, T., Sugawara, I. and Tsuruo, T.: Functional involvement of P-glycoprotein in blood-brain barrier. J. Biol. Chem. 267: 20383–20391, 1992.

Tsuji, A., Terasaki, T., Takabatake, Y., Tenda, Y., Tamai, I., Yamashima, T., Moritani, S., Tsuruo, T. and Yamashita, J.: P-glycoprotein as the drug efflux pump in primary cultured bovine brain capillary endothelial cells. Life Sci. **51:** 1427–1437, 1992.

Wang, Y. and Sawchuk, R. J.: Zidovudine transport in the rabbit brain during intravenous and intracerebroventricular infusion. J. Pharm. Sci. **84:** 871–876, 1995.

Yamaoka, K., Tanigawara, Y., Nakagawa, T. and Uno, T.: A pharmacokinetic analysis program (MULTI) for microcomputer. J. Pharmacobio-Dyn. **4:** 879–885, 1981.

Yano, Y., Yamaoka, K. and Tanaka, H.: A nonlinear least squares program, MULTI(FILT), based on fast inverse Laplace transform for microcomputers. Chem. Pharm. Bull. **37:** 1035–1038, 1989.

Send reprint requests to: Yuichi Sugiyama, Ph.D., Professor, Department of Pharmaceutics, Faculty of Pharmaceutical Sciences, The University of Tokyo, Hongo, Bunkyo-ku, Tokyo 113, Japan.

GLOSSARY

$C_{p,u}$ = unbound serum concentration
f_u = serum unbound fraction
AUC_u = area under the unbound serum concentration-time curve
$PS_{BBB,app}$ = apparent influx clearance across the BBB
$PS_{CSF,app}$ = apparent influx clearance across the BCSFB
PS_{BBB} = symmetrical permeability clearance across the BBB
$PS_{BBB,eff}$ = efflux clearance across the BBB
PS_{CSF} = symmetrical permeability clearance across the BCSFB
$PS_{CSF,eff}$ = efflux clearance across the BCSFB
C_{br} = total brain concentration
C_{ISF} = ISF concentration
C_{CSF} = CSF concentration
$K_{p,u,br}$ = total brain-to-unbound serum concentration ratio ($C_{br}/C_{p,u}$)
$K_{p,u,CSF}$ = CSF-to-unbound serum concentration ratio ($C_{CSF}/C_{p,u}$)
CL_{CSF} = apparent efflux clearance from the CSF
D_t = diffusion coefficient in the brain tissue
D_w = diffusion coefficient in the agar
Mw = molecular weight
V_{br} = distribution volume in brain tissue (C_{br}/C_{ISF})
V_{CSF} = volume of the CSF
Ar = surface area of the ependyma
Q = bulk flow rate of the CSF
L = thickness of the brain cortex